THE JOURNAL OF BIOLOGICAL CHEMISTRY VOL. 285, NO. 47, pp. 36561–36569, November 19, 2010

Crystal Structures of Mutant Forms of the Yeast F_1 ATPase Reveal Two Modes of Uncoupling*[S]

Received for publication, August 11, 2010, and in revised form, September 2, 2010 Published, JBC Papers in Press, September 15, 2010, DOI 10.1074/jbc.M110.174383

Diana Arsenieva, Jindrich Symersky, Yamin Wang, Vijayakanth Pagadala, and David M. Mueller[1]

From the Department of Biochemistry and Molecular Biology, Rosalind Franklin University of Medicine and Science, The Chicago Medical School, North Chicago, Illinois 60064

The mitochondrial ATP synthase couples the flow of protons with the phosphorylation of ADP. A class of mutations, the mitochondrial genome integrity (*mgi*) mutations, has been shown to uncouple this process in the yeast mitochondrial ATP synthase. Four mutant forms of the yeast F_1 ATPase with *mgi* mutations were crystallized; the structures were solved and analyzed. The analysis identifies two mechanisms of structural uncoupling: one in which the empty catalytic site is altered and in doing so, apparently disrupts substrate (phosphate) binding, and a second where the steric hindrance predicted between γLeu83 and β_{DP} residues, Leu-391 and Glu-395, located in Catch 2 region, is reduced allowing rotation of the γ-subunit with less impedance. Overall, the structures provide key insights into the critical interactions in the yeast ATP synthase involved in the coupling process.

The mitochondrial ATP synthase is a molecular motor that couples the transport of protons down a potential gradient with the phosphorylation of ADP. This process can be reversed and the hydrolysis of ATP results in the pumping of protons out of the mitochondrial matrix into the cytoplasm generating a proton gradient. In the synthesis mode, the protomotive force is established by oxidation of NADH or succinate by the electron transport chain. Whereas much is known on the structure/function of the ATP synthase and the mechanism of ATP hydrolysis, less is known on the molecular details on the coupling of proton transport and ATP synthesis. The structure/function relationship of the ATP synthase is key to understanding the coupling mechanism; that is, identification of which intra- and intermolecular interactions within the ATP synthase critical for coupling.

The ATP synthase is composed of two distinct components, the F_1 and the F_o portion and as such is referred to as the F_1F_o ATP synthase. The F_1 portion contains the catalytic sites and is composed of $\alpha_3\beta_3\gamma\delta\epsilon$ with an overall molecular mass of about 350 kDa (1). The active site is composed of the $\alpha\beta$ pair, and thus there are three catalytic sites per complex. The $\gamma\delta\epsilon$-subunits comprise the central stalk with the γ-subunit situated in the middle of the $\alpha_3\beta_3$ subcomplex. The central stalk acts as a rotor and drives conformational changes in the active sites in a sequential manner, thereby effecting ATP synthesis. The δ- and ϵ-subunits are critical for coupling (2, 3), but their roles are unclear, they may participate directly in the coupling process or needed merely for structural purposes.

The F_o portion of the ATP synthase acts as a proton turbine whose rotation is physically coupled to the central stalk and drives its rotation. F_o is minimally composed of subunits abc_{10} with the c_{10} arranged as a cylinder within the membrane (4). Subunit a is thought to directly participate in the proton flow while subunit b is minimally involved in the structure of the peripheral stalk. The peripheral stalk is composed of subunits b, d, h, and subunit 5 (5–8) and acts as a stator connecting F_1 with F_o thereby preventing futile rotation of F_1 without ATP synthesis. Thus, simply based on the structure of the ATP synthase, these subunits are essential for either the structure, the catalytic mechanism or for the coupling mechanism. It is not certain which subunits participate directly in transforming the energy of rotation of the central stalk to the phosphorylation of ADP.

There are three regions in the F_1 ATPase that are highly pertinent to the coupling of the ATP synthase: the collar, Catch 1 and Catch 2 (1). The collar is formed by residues in the α- and β-subunits and encircles the γ-subunit presumably to fix the axis of rotation. Catch 1 and Catch 2 are in the β-subunits and residues within form contacts with the γ-subunit, which in part, define the structure of the active site.

A number of mutations have been isolated in yeast *Kluyveromyces lactis* that allow the cells to lose their mitochondrial DNA and as such, were named mitochondrial genome integrity (*mgi*)[2] mutations (9–12). Surprisingly, *mgi* mutations were mapped to the α-, β-, or γ-subunits of the ATP synthase. Similar, if not identical, mutations were identified using a similar selection scheme in yeast *Saccharomyces cerevisae* (13) and in a related approach using the blood form of *Trypanosoma brucei* (14). While the relationship between the effect of the mutations and the resulting phenotypes is still unclear, there is good biochemical and genetic evidence that when the corresponding mutations are present in the yeast ATP synthase, the enzyme is uncoupled (15). The distinction should be made that these mutations do not simply inhibit the phosphorylation of ADP to ATP, but the mutations reduce the efficiency of ATP synthesis

* This work was supported, in whole or in part, by National Institutes of Health Grant National Institutes of Health R01GM66223 (to D. M. M.).

The atomic coordinates and structure factors (codes 3OEE, 3OEH, 3OFN, and 3OE7) have been deposited in the Protein Data Bank, Research Collaboratory for Structural Bioinformatics, Rutgers University, New Brunswick, NJ (http://www.rcsb.org/).

[S] The on-line version of this article (available at http://www.jbc.org) contains supplemental Tables S1–S3, Figs. S1–S5, and Movies S1–S4.

[1] To whom correspondence should be addressed: 3333 Green Bay Rd., North Chicago, IL 60064. Fax: 847-578-3240; E-mail: david.mueller@rosalindfranklin.edu.

[2] The abbreviations used are: *mgi*, mitochondrial genome integrity; AMP-PNP, 5′-adenylyl-β,γ-imidodiphosphate; TF1, Thermophile F_1.

by allowing proton flow without ATP synthesis, *i.e.* the mutations uncouple this process.

The high-resolution crystal structure of the bovine ATPase has been determined for a number of different states (1, 16–24) and for the yeast enzyme in the presence or absence of bound nucleotides (16, 17). Here we report the structures of yeast F_1 ATPase with four *mgi* mutations. The mutant enzymes crystallized under similar conditions as the wild type enzyme, and as such, there are three enzyme complexes in the asymmetric unit, which represent two different states of the enzyme and thus 8 unique F_1 structures. These structures represent the first crystallographic study on mutant forms of the F_1 ATPase and provide the first structural insights into how mutations uncouple the ATP synthase. These studies identify critical regions within the ATP synthase that are involved in the coupling process.

EXPERIMENTAL PROCEDURES

Yeast Growth, Purification, and Crystallization of F_1 ATPase Mutants—The yeast strains (15), growth conditions (18), purification, and crystallization (16, 18, 19) were described previously. Briefly, genetically engineered yeast strains were used with a hexahistidine tag on the N terminus of the β-subunit of the F_1 ATPase. The mutant F_1 ATPase was purified after release from submitochondrial particles with chloroform, by a combination of Ni^{2+}-chelate affinity chromatography and gel filtration and crystallized using polyethylene glycol 6000 in conditions similar to that of the wild type F_1 ATPase (16, 19).

Data Collection and Refinement—Diffraction data were collected at 100 K in oscillation mode at the Advanced Photon Source, beamline GM/CA-CAT 23ID, using single wavelengths from 0.96–1.03 Å. Diffraction images were integrated and scaled in HKL2000 (21). Molecular replacement was performed in MOLREP (22) with the search model consisting of chains A-I from the yeast F_1 ATPase structure (16), PDB code 2HLD. The structural models were refined in REFMAC5 (23) using rigid-body, restrained, and Translation/Libration/Screw (TLS) refinement. Electron density maps were calculated in CCP4 (24), the models were rebuilt in COOT (25) and validated in PROCHECK (26). The Ramachandran plots showed on average 88.4% residues in most favored regions, 11.6% in additional regions, and 0.0% in disallowed regions (supplemental Table S1).

Structure Analysis—A truncated model consisting of the β-barrel regions of wild type complex yF_1II (residues 26–96 of α-subunits and 10–80 of β-subunits) was placed on principal axes by using AMORE (27). Complete models of all complexes were overlaid on this truncated model using SUPERPOSE (24), using the α-carbon atoms of respective β-barrel regions. All models were rotated around the common central principal axis to desired degree of rotation with PDBSET (24). To determine the degree of rotation of the γ-subunit in various complexes (supplemental Table S2), the γ-subunit of each structure was rotated around the central axis in 1^o increments. After each step, the γ-subunit was compared with the reference structure (γ-subunit of wild type yF_1I). The rotation angle was defined as the position that had the lowest centroid distance as measured between residues 18 and 25 of γ-subunit (SUPERPOSE, Ref. 24). Residues 18–25 of the γ-subunit were chosen because this region is involved in critical contacts with residues that help define the active site.

The Evolutionary Trace Server (28) was used to find and align sequences of α-, β-, and γ-subunits to determine the conservation of the amino acid residues in the F_1 ATPase. The figures containing molecular models were made using Pymol (29). Coordinates and structure factors have been deposited in the Protein Data Bank with accession codes 3OEE, 3OEH, 3OFN, 3OE7.

RESULTS

The high resolution structure of the bovine enzyme (1) established the naming convention of the three active sites in F_1: DP, TP, and E, where DP refers to the ADP-bound site, TP refers to the ATP (or AMP-PNP)-bound site, and E refers to the catalytic site that has no nucleotide bound. Regardless of the occupancy of the catalytic site in the current or prior models, the naming convention is continued as the active site is distinguished by a number of other features, most principally, the relative position of the γ-subunit. The β-subunits that form the active sites are referred to as β_{DP}, β_{TP}, and β_E with analogous convention for naming the α-subunit that pairs with the β-subunit to form the active site, α_{DP}, α_{TP}, and α_E. The interacting α/β pair that forms the DP, TP, or E sites will be referred to as the DP, TP, or E pair.

The yeast enzyme crystallized with three F_1 complexes in the asymmetric unit, heretofore referred to as yF_1I, yF_1II, and yF_1III. yF_1I and yF_1II are thought to represent two different catalytic states of F_1 (16). While both yF_1I and yF_1II contain AMP-PNP in the DP and TP sites, yF_1II has phosphate bound to the E site, which is associated with differences in the twisting of the γ-subunit. The structure of yF_1II identified the residues involved in binding phosphate (16). yF_1II likely represents the structure of the yF_1 with one of the substrates for ATP synthesis, phosphate, bound to the active site.

The α- and β-subunits share structural homology. Up to the first 96 residues of the α- and 80 residues of the β-subunit, comprise a β-barrel structure. The structure of the β-barrel domain does not change significantly between the different catalytic forms and thus serves as a good reference point for structural alignment. The middle core region comprises the nucleotide binding sites, noncatalytic for the α-subunit and catalytic for the β-subunit. The conformations of DP and TP catalytic sites are nearly identical, while that of the E site differs considerably. The lower third of each subunit is composed of an α-helix bundle. Many of the helices in these regions are in different positions depending on the catalytic cycle, but also tend to be most variable between various structures of the bovine and yeast F_1 ATPase.

Fig. 1 (and supplemental Movie S1) shows the position of the residues (αAsn67, αAla295, αPhe405, βVal279, βArg408, γThr264, and γIle270), in the structure of the wild-type F_1 that were identified in the *mgi* selection. The relative positions of these residues and bound phosphate are shown. For reference, the collar regions are α287–299 and β272–284, Catch 1 is β309–320, and Catch 2 is β386–400.

Fig. 1*A*, shows residue αAsn67 is in the β-barrel region of the α-subunit, which lies above the collar region. In the E and DP pairs, αAsn67 forms two H-bonds with αArg289, which is in

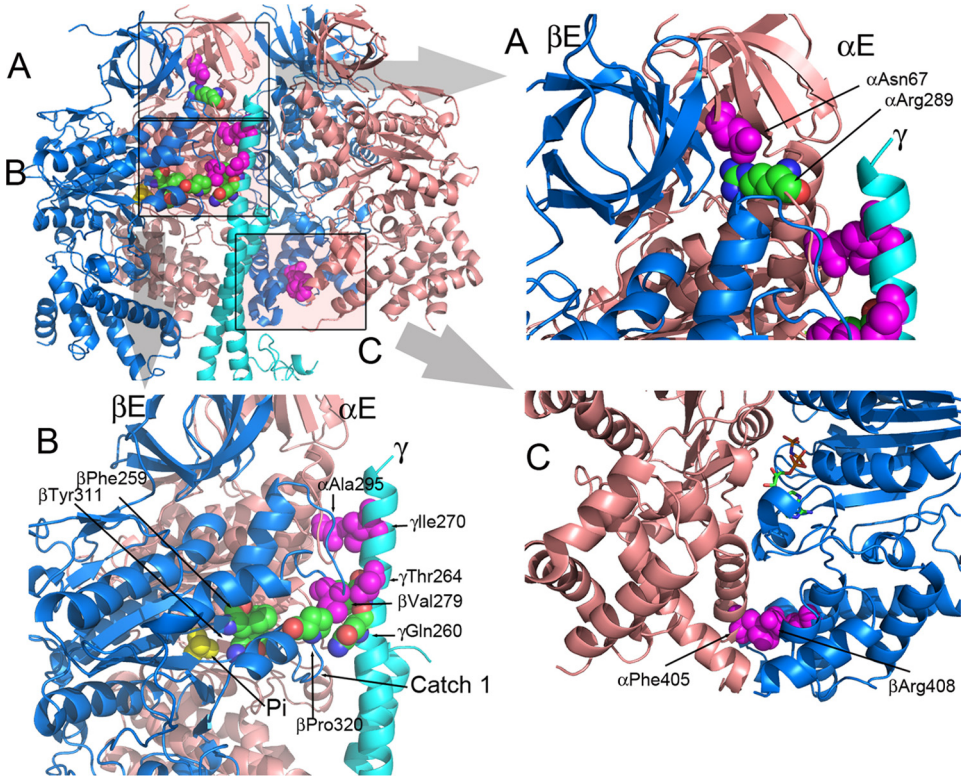

FIGURE 1. **Positions of the *mgi* residues in the structure of the yeast F_1 ATPase.** The *mgi* residues are colored *magenta*, and the atoms are shown as *spheres*. The atoms of interacting residue are shown as *spheres* but colored as defined by the atom type. The panel in the *upper left* shows a cartoon representation of the α- (*salmon*) and β- (*blue*) subunits forming the E and DP sites along part of the γ-subunit (*light blue*). In the *upper left panel*, the areas shaded and labeled as *A*, *B*, and *C* represent the regions shown in *A*, *B*, and *C*. *A*, the region illustrates the *mgi* residue, αAsn67 and its interaction with αArg289. *B*, *mgi* residues, αAla295 and γIle270 form interacting pairs, along with βVal279 and γThr264. Phosphate (P_i) is shown in *yellow*. αAla295 is located in the collar region of the α-subunit, and βVal279 is in the collar region of the β-subunit. βPhe259 and βTyr311 are critical interacting pairs that aid in forming the active site. *C*, *mgi* residues αPhe405 and βArg408 make critical contacts in TP and DP pairs of yF_1II, but not yF_1I. The nucleotide is shown as a *stick model* in atom-defined colors.

the collar region. Fig. 1*B* and supplemental Movie S1, show that residues αAla295, βVal279, γIle270, and γThr264 face the E pair and not the DP or TP pairs. Residues αAla295 and γIle270 form interacting pairs, as do βVal279 and γThr264. Residues αAla295 and βVal279 are in the collar region of the F_1, which is just above the Catch 1 region of the β-subunit. In the TP pair, αAla295 is adjacent to γThr264. Finally, residues αPhe405 and βArg408 (Fig. 1*C*) were both identified in the *mgi* screen and are located at the interface of the α- and β-subunits in the α-helix bundle domains. In the DP pair of yF_1II, but not yF_1I, the side chains of αPhe405 and βArg408 interact with each other through cation/π interaction.

Four mutant forms of the yeast F_1 ATPase with corresponding *mgi* mutations were crystallized and the structures were determined: αAsn67Ile, αPhe405Ser, βVal279Phe, and γIle270Thr. These mutations reduce, but do not eliminate, the coupling of the ATP synthase (15). Supplemental Fig. S1 shows composite omit density map in the area surrounding each mutated residue, which supports the contention that these are indeed the mutant forms of the enzyme.

The crystallographic data are presented in supplemental Table S1. The resolution of the structures varied from 2.7 Å (for αPhe405Ser) to 3.2 Å (for αAsn67Ile and γIle270Thr). Like the wild-type enzyme, the mutant forms of the enzymes crystallized in $p2_1$ space group with three F_1 complexes in the asymmetric unit. As with the wild-type structure, the electron density of yF_1I is better on an average than that of yF_1II, and much better than that of yF_1III. The structure of yF_1III is similar to that of yF_1I and thus, will not be discussed.

Structure of Wild Type yF_1I versus yF_1II—In the wild-type enzyme, the structures of yF_1I and II differed in three principle ways (Summarized in supplemental Fig. S2). First, the γ-subunit is twisted by about 17° in the direction of ATP hydrolysis (based on residues 18–25 in the γ-subunit, counterclockwise as viewed from the foot of the stalk) in yF_1I relative to that of yF_1II. Secondly, in yF_1II, phosphate is bound to β_E in a site that is consistent with being the substrate binding site, and thus the structure represents a catalytic intermediate. Presumably, this structure represents the catalytic intermediate where substrate, phosphate but not ADP, is bound to the active site. It is not clear if phosphate binding induces the twisting of the γ-subunit or if the twisting of the γ-subunit promotes the binding of phosphate.

A third difference between yF_1I and yF_1II with the wild-type enzyme is that in yF_1I, the interface between the α- and β-subunits in the DP pair is more open in yF_1I as compared with that of yF_1II. This effect is most pronounced in the C-terminal helical domain, which contains the Catch II region. The significance of this difference is discussed later in the context of the results from this study.

Structure of Mutant Forms of yF_1I versus yF_1II—The structural differences between yF_1I and yF_1II in the structures of the wild type enzyme were not consistently observed with each of the structures of the mutant forms (Summarized in supplemental Table S2). One surprising difference is that for the mutant form of αAsn67Ile, the structures of yF_1I and yF_1II are similar showing little differences in the twisting in the γ-subunit and phosphate was not bound to E site of yF_1II (supplemental Fig. S2 and Table S2). Minimally, this suggests that the crystal contacts in yF_1II do not cause the differential twisting of the γ-subunit and suggests that the binding of phosphate is required for the twisting of the γ-subunit.

In the structures of yF_1II for both αPhe405Ser and βVal279Phe, the γ-subunit is twisted in the same manner as the wild-type γ-subunit, but phosphate is not bound to the phosphate-binding site in the E site. (There is electron density adjacent to the P-loop in yF_1I and yF_1II of αPhe405Ser, which could be phosphate or sulfate (supplemental Fig. S3). However, this is

not in the normal phosphate binding site (16) and its nature is unclear.) Further, the twisting of the γ-subunit in γIle270Thr of yF_1II is very similar to that of yF_1II of the wild-type enzyme and in this case, phosphate is bound to the E site. Taken together, these results suggest that phosphate-binding neither dictates, nor is determined by, the twisting of the γ-subunit. However, these results are all in the context of mutations that alter the coupling of the ATP synthase and the *mgi* mutations may have differentially affected the relationship between phosphate binding and the twisting of the γ-subunit. If correct, then this may in part, explain the uncoupling effect of some of the *mgi* mutations.

As stated earlier, the interface between the α- and β-subunits in the DP pair in the wild-type structure is more open in yF_1I as compared with that of yF_1II. For comparison, the distances were measured between the Cα carbons of αPhe405 and βArg408. These residues are at the exterior and within the C-terminal helical domains and both have been identified as residues that are mutated in the *mgi* class of mutations (9–11, 30). For the wild type enzyme, the distance in yF_1I was 15.6 Å, while that in yF_1II was reduced to 10.9 Å. Thus, the DP pair is more closed in yF_1II as compared with yF_1I, in the wild-type enzyme. The DP pairs in yF_1II were also more closed for the structures of the mutant forms of βVal279Phe and γIle270Thr, but not in the structures of the mutant forms of αPhe405Ser and αAsn67Ile where the DP pairs in yF_1II were more open, comparable to the DP pair in yF_1I. The more open DP pair in yF_1II of αPhe405Ser is not surprising, because αPhe405 interacts with βArg408 in the DP pair of yF_1II and is partly responsible for the stabilization of the closed form of the DP pair in yF_1II (Fig. 1*C*). The more open structure is also expected for the structure of the mutant form of αAsn67Ile as in this structure, yF_1II is nearly identical to that of yF_1I, with little difference in the twisting of the γ-subunit. Lastly, the result is consistent with the structure of the mutant form of γIle270Thr, whereas in this structure, the E site of yF_1II has bound phosphate and the γ-subunit is twisted in yF_1II as in the wild-type structure, *i.e.* the structure is largely unchanged from the wild-type structure.

The DP/TP/E active sites in yF_1I and the TP active sites of yF_1II of the mutant structures are not altered as compared with the corresponding active sites in the wild type enzyme. Also, despite the change in the α/β interface of the DP pair in two of the mutant forms in yF_1II, the DP active sites were not largely changed in comparison to those of the wild type yF_1II. (There were some minor changes as discussed below.) In contrast, the structure of the E active site of yF_1II shows changes in two of the structures, suggesting a role of the E site in the coupling mechanism.

αAsn67Ile Alters the Phosphate Binding E Catalytic Site—αAsn67 is located at the top of F_1 in the β-barrel domain and is about 7.4 Å from αLeu287 (Cα carbon to Cα carbon) located at the beginning of the collar region (Fig. 2). Residue, αAsn67 is linked to the collar by two H-bonds with αArg289, which is located at the top of the collar region of the α-subunit just after Helix D. These hydrogen bonds are present in the E and DP pairs, but not in the TP pair, and as such, the conformation of the TP pair did not change in the mutant structure of αAsn67Ile in either yF_1I or yF_1II. There were some structural changes in

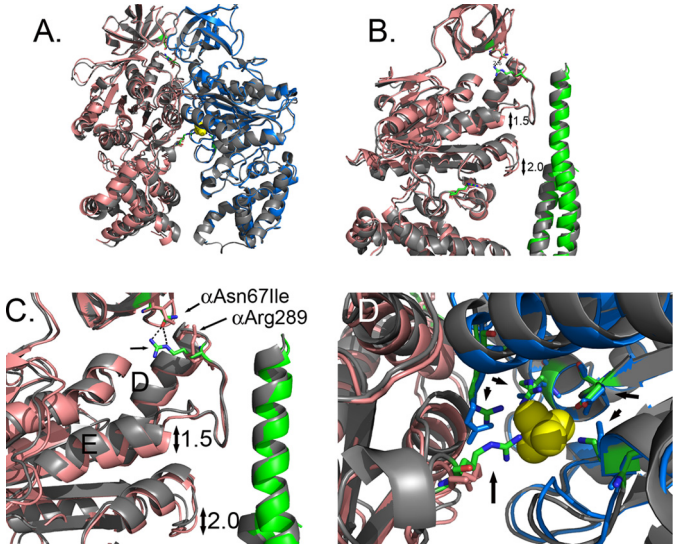

FIGURE 2. **Structural changes observed in the F_1 structure with *mgi* mutation, αAsn67Ile.** *A* shows an overlap of the E site α- and β-subunits form the wild type (*gray*) and αAsn67Ile structure. The α- and β-subunits of the mutant structure are shown in *salmon* and *blue*, respectively. *B* is a closer view showing the shifts in the position of the helix following the collar region and the region in the α-subunit that is the structural analog to the Catch 1 region of the β-subunit. The wild-type γ-subunit is colored *gray*, and the mutant structure is colored *green*. *C* shows the disruption of the H-bond between αAsn67 and αArg289 with the αAsn67Ile mutation. The residues are shown in *stick representation* with the wild type colored as defined by the atom. *D* shows a view of the phosphate binding site and the relative changes in the atom positions with phosphate shown in *yellow*. The atoms of the wild-type structure are colored as defined by the atom. The residues indicated by the *arrows* correspond to: αArg375, βArg190, βArg260, βAsp256, and βLys163 (P-loop) starting at the bottom and proceeding in a clockwise direction.

both the E and DP catalytic sites, for yF_1I or yF_1II, but the changes were more profound for the E site than those in the DP site. For the E catalytic site, the conformational differences were larger in yF_1II than those in yF_1I. Fig. 2*A* shows an overlap of the α- and β-subunits from yF_1II from the wild-type enzyme and that of αAsn67Ile using the β-barrel domains as the reference point. While the structures of the β-subunits nearly perfectly superimposed, the α-carbons of the corresponding α-subunits were displaced. The hydrogen bonds between αAsn67/αArg289 were broken in the mutant structure, which resulted in a displacement of the α-helices in the nucleotide binding domain and the α-helical bundle (Fig. 2, *B* and *C*). The movements in the helices of the nucleotide binding domain are considered more significant than those in the α-helical bundle because these aid in forming the catalytic site at the interface of the α- and β-subunits. In the nucleotide binding domain of the α-subunit, there were shifts of 1.5 Å in Helix E immediately following the collar region and 2.0 Å in the loop that is the structural analog of Catch 1 of the β-subunit. In the E catalytic site, largely formed by the β-subunit, the shifts in the α-subunit disrupted the phosphate-binding site such that the side chain of αArg375 and βLys163 (P-loop) are disordered and the guanidinium group of βArg190 is displaced by 1.7Å (Fig. 2*D*). The remaining residues that contribute to phosphate-binding, βAsp256 and βArg260, are well ordered and in the same position relative to the wild-type structure. Movements in the catalytic site residues that bind phosphate may explain the absence of phosphate in the E site of yF_1II.

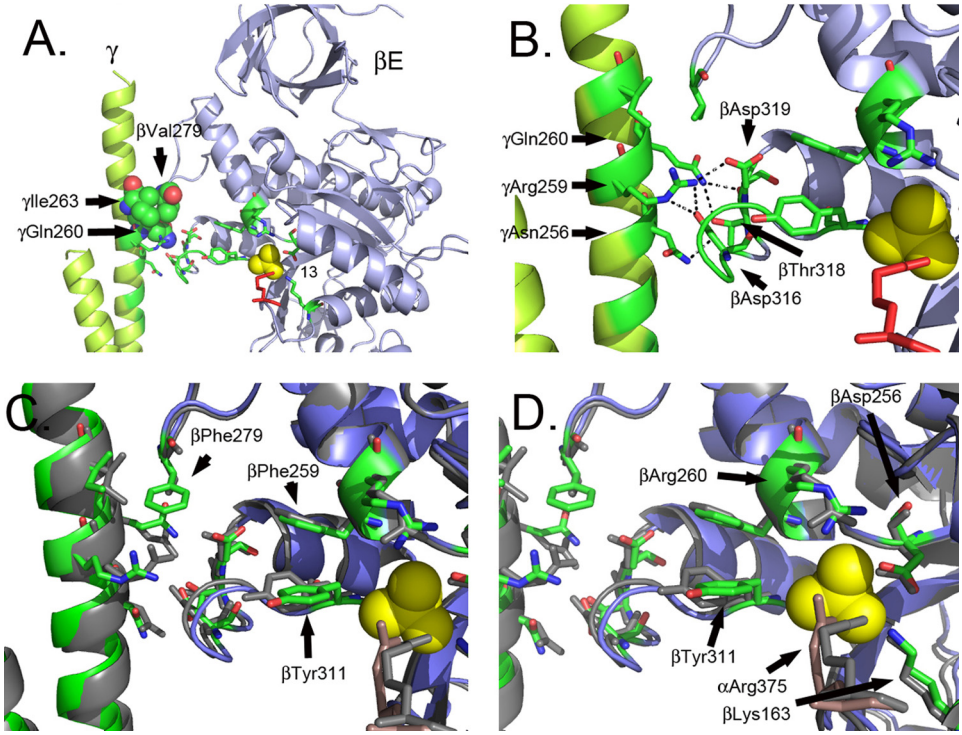

FIGURE 3. **Structural changes observed in the F_1 structure with *mgi* mutation, βVal279Phe.** *A* and *B* show the structure of the β- and γ-subunits of wild-type F_1 from yF_1II. *A* shows a position of βVal279 and the interacting residues on the γ-subunit. *B* shows the interactions in the Catch 2 region between the residues of the β- and γ-subunits. The atoms colored in *red* correspond to αArg375. *C* and *D* show an overlap of the wild type (*gray*) and mutant structures (*green* and *blue*) and the relative shifts in positions. The atoms colored in *dark salmon* correspond to αArg375. The shift in the residues eliminates the H-bonds in the Catch 1 region in the mutant structure, and phosphate is not bound in the mutant structure.

βVal279Phe Alters Catch 1 Interactions and the Phosphate Binding Site—Residue βVal279 is located in a loop (residues 272–284), which together with a loop in the α-subunit (residues 287–299), form a collar, which encircles the γ-subunit (supplemental Fig. S4). The collar is formed by six loops: three from the α-subunit and three from the β-subunit. The C terminus of the γ-subunit forms an α-helix, which is curved and encircled by the collar. The apexes of the six loops that form the collar are not in the same plane, but rather step into different planes as the γ-subunit rotates. The stepping movement of the loops is necessary to keep the rotation of the γ-subunit along a fixed axis since the γ-subunit is curved. The collar is a rather rigid structure as seen by the phi-psi angles, and the presence of proline residues, which suggests that the collar limits wobble during rotation of the γ-subunit.

In β_E of yF_1II, β_EVal279 forms three hydrophobic or van der Waals contacts with γIle263 and is within 3.8 Å of γGln260) (Fig. 3*A*). There is also a contact between the amide nitrogen of β_EVal279 and the side-chain hydroxyl of γThr264 (3.1 Å), though the geometry is not ideal for a strong H-bond. These interactions likely aid in defining the structure of this region, but also define the steric limits of β_EVal279 with the γ-subunit. Importantly, γThr264Ala has been identified as an *mgi* mutation.

In addition to the collar region, there are two regions in the β-subunit that make close contacts with the γ-subunit and these are referred to as Catch 1 and Catch 2 (1). Catch 1 is located in the loop that extends from β_EAla309 to β_EPro320 and follows β-sheet 13 where residues in β_E form H-bonds with residues in the γ-subunit: β_EAsp316, β_EThr318, β_EAsp319 and γArg259 and γAsn256 (Fig. 3*B*). Also located in the loop is β_ETyr311, which apparently forms π-π interactions with β_EPhe259. Residue, β_EPhe259, is immediately adjacent to β_EArg260, which forms part of the phosphate-binding site in β_E (Fig. 3*B*) (17). Thus, there is a possible conformational relay in β_E from the collar region to the phosphate-binding site via Catch 1.

The side chain of β_EVal279, is located about 3.6 Å from the side chain of β_EPro320 located at the beginning the loop that contains Catch I and is adjacent to γIle263 (Fig. 3, *A* and *B*). A principal effect of the βVal279Phe mutation on the structure of the F_1 ATPase is that the larger phenylalanine side chain causes a movement in the position of the γ-subunit such that the axis of the γ-subunit is translated away from the β_E-subunit (Fig. 3, *C* and *D*) and in doing so, disrupts the H-bonding network between residues in Catch 1: β_EAsp316 and γAsn256, β_EAsp316, and γArg259, βAsp319, and γArg259, β_EThr318 and γGln260 and α_{TP}Asp355 and γArg257 (supplemental Table S3 and Movie S2). All of the H-bonds are either weakened or destroyed, as is the case for β_EAsp319 and γArg259, which is moved by more than 2 Å to a distance of 5.1 Å. The H-bonding network in Catch 1 is more extensive in yF_1II as compared with yF_1I, but in both cases, the mutation βVal279Phe weakens or eliminates the H-bonds. The loss of the H-bonds in the Catch 1 region has an effect on the phosphate-binding site where there are movements in critical side chains involved in phosphate-binding including β_EArg260 and β_EAsp256. Like the αAsn67Ile mutation, the E site does not have phosphate bound, likely due to the shifts in the critical side chains involved in phosphate-binding.

γIle270Thr Alters Hydrophobic Interactions at the E Pair Interface—Residue, γIle270, is nearly at the end of the γ-subunit and lies just 2 α-helical turns from the C terminus (Figs. 1, *A* and *B* and supplemental S5). Consistent with the interactions observed with β_EVal279 and the γ-subunit, γIle270 interacts with residues in the E pair, but here with α_E, which is adjacent to β_E. Residue, α_EAla295 interacts with γIle270, which is located in the γ-subunit on the same face of the α-helix as γLeu267. The face of the α-helix in this region of the γ-subunit is hydrophobic and highly conserved across species, while the opposite face is hydrophilic and not highly conserved. Interestingly, the same residue, αAla295 in α_{TP}, interacts with γThr264 and mutations in each of these residues, α_{TP}Ala295, γIle270, and γThr264, have been identified as *mgi* mutations (Fig. 1) signifying a com-

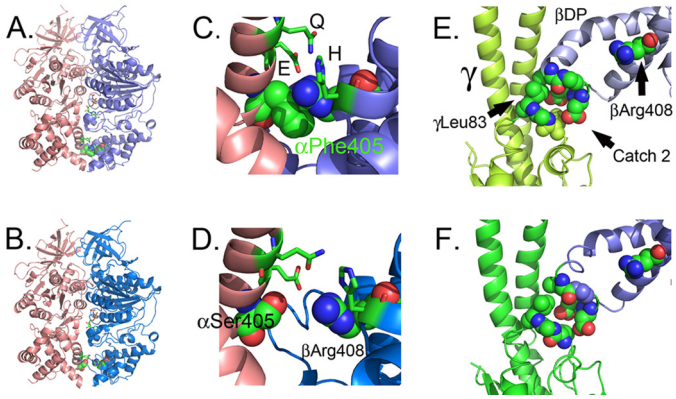

FIGURE 4. **Structural changes observed in the F_1 structure with *mgi* mutation, αPhe405Ser.** *A*, *C*, and *E* correspond to the structure of the DP site from wild-type F_1, while *B*, *D*, and *F* correspond to the structure of the DP site with αPhe405Ser. The structures were overlapped and represent the same views, *A* and *B*, *C* and *D*, and *E* and *F*. The α-, β-, and γ-subunits are colored in *salmon*, *blue*, and *green*, respectively. *A* and *B* show the change in the association between the α- and β-subunits as a result of the mutation. *C* and *D* show the same but with a closer view of the *mgi* residues, βArg408 and αPhe405, or the mutation αPhe405Ser (*D*), shown as *spheres*. The residues shown as *sticks* also contribute to the closed conformation of the DP pair and correspond to βGlu401 (*E*), βGln398 (*Q*), and βHis455 (*H*). *E* and *F* show the interaction of Catch 2 with the γ-subunit along with the neighboring and interacting residues, in a *space-filled model*. The electron density for the side chain atoms for the mutant structure for γLeu83 is weak in *F*, indicating disorder, but not so in the structure of the wild type, *E*.

mon functional importance of these residues with regard to their position on the γ-subunit and their interactions with the E pair of F_1.

Residue, α_{TP}Ala295 is in the collar, which is formed by residues 287–299 of the α-subunit and 272–284 of the β-subunit. The main chain atoms, and the side chain C atom of α_EAla295 are within 4 Å of the atoms in γ-Ile270. Similarly, atoms of α_{TP}A295 are within 3.9 Å of atoms of γThr264. Thus, while these contacts do not seem to provide strong positive interactions, the predicted rigid structure of the collar region is expected to keep the rotation of the γ-subunit along a tight axis as movements outside the axis would result in repulsive van der Waal forces.

The mutation, γIle270Thr, shows little effect on the structure of the F_1 ATPase. There is little distortion observed in the structure of the α-, β-, or γ-subunits in the immediate region or beyond. This is consistent with the replacement of the larger side chain of Ile for the smaller side chain of Thr. This replacement, instead of distorting the structure, provides a less hydrophobic interface with the α_{TP} and reduces the packing. The result is that the shortest distance between atoms of γIle270Thr and α_E-Ala295 increases from about 3.4 Å to 4.1 Å. This change can have a significant effect on the van der Waals repulsive forces (a function of r^{-6}) and thus the axis of rotation.

αPhe405Ser Alters the Structure of the DP α-Helical Domain—Residue αPhe405 is in the α-helical bundle at the bottom of F_1 and at the interface with the β-subunit. In the DP pair of yF_1II, but not yF_1I, αPhe405 forms a contact with βArg408 causing the interface to close (Fig. 4, *A* and *C*). The mutation, αPhe405Ser, disrupts this interaction and results in a more open interface more closely resembling DP pair of yF_1I (Fig. 4, *B* and *D* and supplemental Movie S3). αPhe405 is one of a number of residues, including βHis455, αGlu401, βArg408, and αGln398, which form a series of interactions that close the interface between the α- and β-subunit in the DP pair of yF_1II.

αPhe405 is 21 Å from the bound nucleotide in the DP and TP sites. The opening of the α/β interface in yF_1II by the αPhe405Ser mutation is transmitted to the DP site causing a slight movement of the α-subunit relative to the β-subunit, but the interactions with the bound nucleotide remain intact. Because the αPhe405/βArg408 interaction is not present in the TP pair, there is little effect on the structure of the TP site. Overall, there is little change in either the DP site, and no change in the TP site, caused by the αPhe405Ser mutation.

The DP pair plays a central role in the coupling of the rotation of the central stalk and in the synthesis of ATP. The DP pair abuts against the γ-subunit with β_{DP}Leu391 forming hydrophobic contacts with γLeu83 (Fig. 4*E*). During ATP synthesis, β_{DP} must move to allow rotation of the γ-subunit, as in the absence of this movement, there is a predicted steric clash between γLeu83 and residues located in Catch 2 region, β_{DP}-Leu391 and Glu395 (Fig. 4*E*). The position of the Catch 2 region of the β-subunit in the DP pair may be critical in preventing rotation of the γ-subunit until the appropriate conditions are met in the catalytic sites, *e.g.* ATP synthesis, substrate bound, or product released.

The mutation αPhe405Ser also alters the position of the γ-subunit, the loop of the γ-subunit containing residue γLeu83, and the Catch II loop containing residues β_{DP}Leu391 and βGlu395 (Fig. 4*F* and supplemental Movie S4). There is displacement of about 2 Å between β_{DP}Leu391 and γLeu83 and the side chains of γLeu83 are not as well ordered suggesting movement. These shifts alter the association of β_{DP}Leu391 with γLeu83 and open a gap in the path of the γ-subunit such that the apparent steric clash with the β_{DP} with rotation of the γ-subunit in the direction of ATP synthesis is reduced.

DISCUSSION

Prior studies have implicated *mgi* mutations in reducing the coupling of the ATP synthase thereby reducing the efficiency of proton translocation and ATP synthesis. The decrease in coupling was indicated by an increased State 4 respiration, a reduced respiratory control ratio, and a decrease in the membrane potential effected by either ATP hydrolysis or NADH oxidation (15). The crystal structures in this study are the first crystal structures of mutant forms of the F_1 ATPase and provide the first insight into the structural changes elicited by mutations that apparently uncouple the ATP synthase.

The defining defect in an enzyme that is uncoupled is that there is either rotation of the central stalk without synthesis or proton leakage without rotation. There are a number of different mechanisms that might allow rotation of the γ-subunit without ATP synthesis including distortion of the γ-subunit, loss of one or more interactions that link critical conformational changes involved in coupling, added steric hindrance preventing normal rotation of the γ-subunit, or loss of steric hindrance or positive interactions, which hold the γ-subunit in place when a torque is applied.

The first key insight into the mechanism of the *mgi* mutations is the clustering of the residues mutated (Group 1) at the face of the E pair. Residues γIle270, αAla295, γThr264, and

βVal279 all face the E pair. Though αAsn67 is in the β-barrel domain, it forms two hydrogen bonds with αArg289, which is located in the collar and adjacent to the E site (see Fig. 1). In addition to the common location, four of these residues form interacting pairs: α_EAla295 with γIle270 and γThr264 with β_EVal279. This coincidence of location and the interacting pairs suggest that the mutations in these residues have a common effect on the function, and possibly structure, of the enzyme. The *mgi* residues, αPhe405 and βArg408 (Group 2) are located far from the Group 1 mutations and seem to act differently. αPhe405 and βArg408 are also an interacting pair, but form only in the DP pair of yF_1II. The location of these residues suggests that mutation of these residues alters the coupling in a manner different from the other *mgi* mutations.

The effects of Group 1 mutations are shown in the structures of both αAsn67Ile and βVal279Phe, but most dramatically in the structure of βVal279Phe. The βPhe279 side chain disrupts the Catch 1 region, which is a set of interactions between the γ-subunit and β_E. The βPhe279 side chain distorts the γ-subunit and the Catch 1 region just enough to break the H-bonds and alter the phosphate-binding site. The structure of the wild type yF_1II identified those residues critical in binding phosphate to the E site: αArg375, βLys163, βArg190, βArg260, and βAsp256 (16). Relative to the position of the bound nucleotide or the P-loop, these residues, or the side chains, move in the transition from E to DP (7.2 Å for αArg375). The altered phosphate-binding site may be the cause for the lack of bound phosphate in E of yF_1II in this mutant structure, as well as that of αAsn67Ile, although phosphate is bound in the γIle270Thr mutant structure. The mutations also cause movement in some of the key residues forming the phosphate-binding site. These changes in phosphate-binding site suggest that the uncoupling is at least, in part, due to the defect in phosphate-binding or recognition. An attractive hypothesis is that the Group 1 mutations alter the E site such that during ATP synthesis, there is rotation of the γ-subunit, converting β_E to β_{DP}, without phosphate bound to the E site, thereby diminishing ATP synthesis and lowering efficiency.

The residue γIle270 is on the same face of the E pair as βVal279 and αAsn67, as thus the γIle270Thr mutation is expected to affect the structure and function in a similar manner as αAsn67Ile and βVal279Phe mutations. However, the mutation γIle270Thr showed little change in the structure as compared with that of the wild type enzyme. There are a number of possible explanations for the lack of structural changes, but the most likely is that the structural changes caused by the mutation would be apparent in a different intermediate structure, for instance, with the application of torque to the γ-subunit. This point is illustrated well in the *mgi* mutations studied here, as in two of the four cases, the conformational changes caused by the mutations were seen only in yF_1II, and not yF_1I or yF_1III.

The Group 2 mutations act in a mechanism different from the Group 1 mutations as first indicated by their different location in the enzyme. Rather than being at the top of F_1 near the collar region and associated with the E pair, the Group 2 mutations are located at the α/β interface at the bottom of F_1 in the α-helical domain adjacent to the Catch 2 region. Disruption of the αPhe405/βArg408 interaction in yF_1II of the DP pair results in an opening of the α/β interface, but there is little effect on the structure of the catalytic site in either DP or E. Instead, the mutation alters the critical interactions between the γ-subunit and the Catch 2 region of the β-subunit.

The β_{DP} subunit makes a unique contact with the γ-subunit where residue γLeu83 with a loop, interacts with the Catch 2 region of the β-subunit. During ATP synthesis, the α-helical bundle domain of the β-subunit must move away from the γ-subunit to allow rotation of the γ-subunit past β_{DP}. Rotation of the γ-subunit is impeded by the repulsive van der Waals interaction of the γLeu83 with the Catch 2 of β_{DP}, which is not dependent on the charge of the residues. The movement of β_{DP} is further impeded if the interface between the α- and β-subunits is in the closed conformation, because this would require either breaking the interacting residues between the α- and β-subunits, or require the movement of the α/β pair. The open and closed interface of the α/β DP pair seem to represent different catalytic intermediates as the interface is closed in yF_1II, but open in yF_1I. The αPhe405Ser, or likely a companion mutation in βArg408, causes the α/β interface in the DP pair to open, which alters the geometry of the γ-subunit such that there is a gap between Catch 2 of β_{DP} and γLeu83 (see Fig. 4F). Thus, it is predicted with αPhe405Ser, that with the twisting of the γ-subunit during the rotation of F_o, that the torque applied to the γ-subunit would allow the γ-subunit to slip past β_{DP} before ADP is converted to ATP, or before substrate is bound to the E site, either resulting in lower efficiency of ATP synthesis.

The proposed models for uncoupling integrate some of the essential structural features of the enzyme: Catch 1, Catch 2, and the loop of the γ-subunit containing γLeu83. The Catch 1 and 2 regions have been under intense investigation since their identification from the structure of the bovine F_1 ATPase. The mutation in the *Escherichia coli* enzyme, γMet23Lys, was one of the first mutations identified as uncoupling (31). This mutation is immediately adjacent to the Catch 2 region and was shown to alter binding constant for phosphate by 7-fold with no effect on the binding of ADP (32). While the corresponding mutation in the yeast enzyme has little effect on the function,[3] the mutation in the *E. coli* enzyme and the corresponding effect on phosphate binding is consistent with the effect of the Group 1 mutations proposed from this work.

The residue that corresponds to γThr264 in the *E. coli* enzyme (γThr273), which interacts with βVal279 (βVal265), was mutated to Ala and Val (33) resulting in an enzyme that had no potential induced by ATP hydrolysis and there was a 50% reduction in potential induced by lactate oxidation. These results are most consistent with an uncoupling of the enzyme allowing flow of protons without ATP synthesis. Mutations have also been made in Catch 1 residues in *E. coli* corresponding to yeast residues βAsp316, βThr318, and βAsp319, and these resulted in various effects, including loss of assembly of the F_1 ATPase, elimination of the k_{cat} for ATP hydrolysis by the F_1-ATPase, and lowered or elimination of growth on succinate medium (34). Interestingly, there was not a good correlation

[3] D. M. Mueller, unpublished results.

between growth on succinate medium and the k_{cat} for ATP hydrolysis, suggesting that the *in vitro* result do not accurately reflect the *in vivo* effect. The inability of the cells to assemble the ATP synthase may be due to the trivial reason of a defect in enzyme folding or lowered stability, or it may be related to a more complex cellular response to a mutation that uncouples the enzyme. Loss of the proton potential in the bacterial cell is expected to be lethal to the cells, as is the case with a mutation that uncouples the eukaryotic mitochondrial enzyme. In yeast, the cell survives by eliminating the source of the leak, F_o, by eliminating the mitochondrial DNA, which encodes subunits of F_o and thus stops the proton leak (2, 35, 36). Possibly an analogous situation is occurring in the bacterial cell, which maybe down-regulating expression of the mutant ATP synthase complex that would otherwise uncouple the cell. Thus, the corresponding mutations in the Catch 1 region are consistent with mutations that uncouple the ATP synthase.

There are a number of residues in the α/β DP interface, in addition to βArg408 and αPhe405, which interact to close the interface in the TP and DP pairs. These residues form a H-bonding network, which were the subject of a mutagenesis study using the *E. coli* enzyme (37). Based on the results, Mao *et al.* (37) proposed a model, which integrated a role of the H-bonding network in the coupling process. Mutagenesis of the H-bonding residues and those that correspond to βArg408 and αPhe405 in *E. coli* (βArg398, αPhe406) resulted in various phenotypes, ranging from no effect to complete loss of F_1 on the membrane. Thus, the mutations were allelic specific and the corresponding phenotypes were not directly related to the loss of H-bonds or favorable interactions. The allelic specificity is likely due to the result of the differing amino acid changing the structure of the surrounding region, as well as altering the H-bonding network, as observed in the structure of αPhe405Ser.

The Catch 2 loop (β386–400) of β_E interacts with the γ-subunit. The ^{394}DELSEQD^{400} region is a highly conserved acidic region in the Catch 2, which was thought to be essential (38) and thus has been the subject of many studies. In TF1, the acidic amino acids in the conserved region were replaced with Ala residues resulting in an ATPase activity that decreased to 37% of the wild-type enzyme, but no apparent effect on the ATP driven rotation of the γ-subunit (39). Thus, this loop does not require a single negative residue for normal torque driven by ATP hydrolysis. In the same study, the residue that corresponds to γLeu83 was mutated to Ala and this resulted in 62% of the wild type ATPase activity and 76% of the torque driven by ATP hydrolysis. Thus, this study suggests a modest role of the interaction between γLeu83 and the Catch 2 region in the coupling of the ATP synthase, at least as determined by ATP hydrolysis. The role of the acidic residues was postulated to be important in the interaction with the ϵ-subunit, which corresponds to the mitochondrial δ-subunit (40, 41). If correct, this would suggest a dual role of the Catch 2 region, one that is directly involved in coupling rotation with ATP hydrolysis and another that is involved in interaction with the mitochondrial δ-subunit.

Partly based on the structures of the F_1 ATPase from bovine and yeast, a course-grained plastic network model was used to show the conformational changes in the β-subunit that act on the γ-subunit to generate the torque and drive the rotation of the central stalk (20). The model used the predicted energies of interactions through repulsive van der Waals interactions and attractive electrostatic forces. This analysis identified four regions in the bovine enzyme within the β- and γ-subunits which are largely responsible for the generation of torque: 1) the N- and C-terminal regions of the γ-subunit γ20–25, and γ232–238 (yeast γ20–25, γ237–243), 2) the Catch 2 region in β_E, 3) residues γ252–258 (yeast γ257–263) and the interacting residues in Catch 1 of β_E, and 4) γ75–79 (yeast γ81–85), which interact with Catch 2 in β_{DP}. Consistent with this work, the crystal structures of the yeast F_1 ATPase with *mgi* mutations have implicated Catch 1, Catch 2, and γLeu83 as important for coupling proton flow with the synthesis of ATP.

In conclusion, the *mgi* class of mutations was previously determined to uncouple the ATP synthase. Structural analysis of yeast F_1 ATPase with four *mgi* mutations identifies two classes, Class 1 which alter the phosphate binding site in the E site, and Class 2 mutations which alter the interaction of the γ-subunit with Catch 2 of the β-subunit. These structures give insight into the regions, which are sensitive to disruption and cause uncoupling of the mitochondrial ATP synthase.

Acknowledgments—We thank the continued support and discussion of Drs. Andrew Leslie and John Walker, MRC, Cambridge, UK. Data were collected at GM/CA Collaborative Access Team (GM/CA-CAT) 23-ID beamline at the Advanced Photon Source, Argonne National Laboratory. Use of the Advanced Photon Source was supported by the U.S. Dept. of Energy, Office of Science, Office of Basic Energy Sciences, under Contract Number W-31-109-Eng-38.

REFERENCES

1. Abrahams, J. P., Leslie, A. G., Lutter, R., and Walker, J. E. (1994) *Nature* **370,** 621–628
2. Lai-Zhang, J., Xiao, Y., and Mueller, D. M. (1999) *EMBO J.* **18,** 58–64
3. Duvezin-Caubet, S., Caron, M., Giraud, M. F., Velours, J., and di Rago, J. P. (2003) *Proc. Natl. Acad. Sci. U.S.A.* **100,** 13235–13240
4. Stock, D., Leslie, A. G., and Walker, J. E. (1999) *Science* **286,** 1700–1705
5. Carbajo, R. J., Silvester, J. A., Runswick, M. J., Walker, J. E., and Neuhaus, D. (2004) *J. Mol. Biol.* **342,** 593–603
6. Dickson, V. K., Silvester, J. A., Fearnley, I. M., Leslie, A. G., and Walker, J. E. (2006) *EMBO J.* **25,** 2911–2918
7. Walker, J. E., and Dickson, V. K. (2006) *Biochim. Biophys. Acta* **1757,** 286–296
8. Rees, D. M., Leslie, A. G., and Walker, J. E. (2009) *Proc. Natl. Acad. Sci. U.S.A.* **106,** 21597–21601
9. Chen, X. J., and Clark-Walker, G. D. (1993) *Genetics* **133,** 517–525
10. Chen, X. J., and Clark-Walker, G. D. (1995) *EMBO J.* **14,** 3277–3286
11. Chen, X. J., and Clark-Walker, G. D. (1996) *Genetics* **144,** 1445–1454
12. Chen, X. J., Hansbro, P. M., and Clark-Walker, G. D. (1998) *Mol. Gen. Genet.* **259,** 457–467
13. Weber, E. R., Rooks, R. S., Shafer, K. S., Chase, J. W., and Thorsness, P. E. (1995) *Genetics* **140,** 435–442
14. Schnaufer, A., Clark-Walker, G. D., Steinberg, A. G., and Stuart, K. (2005) *EMBO J.* **24,** 4029–4040
15. Wang, Y., Singh, U., and Mueller, D. M. (2007) *J. Biol. Chem.* **282,** 8228–8236
16. Kabaleeswaran, V., Puri, N., Walker, J. E., Leslie, A. G., and Mueller, D. M. (2006) *EMBO J.* **25,** 5433–5442
17. Kabaleeswaran, V., Shen, H., Symersky, J., Walker, J. E., Leslie, A. G., and Mueller, D. M. (2009) *J. Biol. Chem.* **284,** 10546–10551
18. Mueller, D. M., Puri, N., Kabaleeswaran, V., Terry, C., Leslie, A. G., and

Walker, J. E. (2004) *Protein Expr. Purif.* **37,** 479–485
19. Mueller, D. M., Puri, N., Kabaleeswaran, V., Terry, C., Leslie, A. G., and Walker, J. E. (2004) *Acta Crystallogr. D. Biol. Crystallogr.* **60,** 1441–1444
20. Pu, J., and Karplus, M. (2008) *Proc. Natl. Acad. Sci. U.S.A.* **105,** 1192–1197
21. Otwinowski, Z., and Minor, W. (1997) *Methods Enzymol.* **276,** 307–326
22. Vagin, A., and Teplyakov, A. (2010) *Acta Crystallogr. D. Biol. Crystallogr.* **66,** 22–25
23. Murshudov, G. N., Vagin, A. A., Dodson, E. J. (1997) *Acta Crystallogr. D.* **53,** 240–255
24. Collaborative_Computational_Project. (1994) *Acta Crystallogr. D.* **50,** 760–763
25. Emsley, P., and Cowtan, K. (2004) *Acta Crystallogr. D. Biol. Crystallogr.* **60,** 2126–2132
26. Laskowski, R. A., MacArthur, M. W., Moss, D. S., and Thorton, J. M. (1993) *J. Applied Crystallogr.* **26,** 283–291
27. Navaza, J. (2001) *Acta Crystallogr. D. Biol. Crystallogr.* **57,** 1367–1372
28. Innis, C. A., Shi, J., and Blundell, T. L. (2000) *Protein Eng.* **13,** 839–847
29. DeLano, W. L. (2002) *The PyMOL Molecular Graphics System*, Delano Scientific, San Carlos
30. Chen, X. J., and Clark-Walker, G. D. (1999) *Mol. Gen Genet.* **262,** 898–908
31. Shin, K., Nakamoto, R. K., Maeda, M., and Futai, M. (1992) *J. Biol. Chem.* **267,** 20835–20839
32. Al-Shawi, M. K., Ketchum, C. J., and Nakamoto, R. K. (1997) *Biochemistry* **36,** 12961–12969
33. Boltz, K. W., and Frasch, W. D. (2005) *Biochemistry* **44,** 9497–9506
34. Greene, M. D., and Frasch, W. D. (2003) *J. Biol. Chem.* **278,** 51594–51598
35. Mueller, D. M. (2000) *J. Bioener. Biomem.* **32,** 391–400
36. Xiao, Y., Metzl, M., and Mueller, D. M. (2000) *J. Biol. Chem.* **275,** 6963–6968
37. Mao, H. Z., Abraham, C. G., Krishnakumar, A. M., and Weber, J. (2008) *J. Biol. Chem.* **283,** 24781–24788
38. Ketchum, C. J., Al-Shawi, M. K., and Nakamoto, R. K. (1998) *Biochem. J.* **330,** 707–712
39. Hara, K. Y., Noji, H., Bald, D., Yasuda, R., Kinosita, K., Jr., and Yoshida, M. (2000) *J. Biol. Chem.* **275,** 14260–14263
40. Yagi, H., Kajiwara, N., Tanaka, H., Tsukihara, T., Kato-Yamada, Y., Yoshida, M., and Akutsu, H. (2007) *Proc. Natl. Acad. Sci. U.S.A.* **104,** 11233–11238
41. Hara, K. Y., Kato-Yamada, Y., Kikuchi, Y., Hisabori, T., and Yoshida, M. (2001) *J. Biol. Chem.* **276,** 23969–23973